Removal of CPR Artifacts from the Ventricular Fibrillation ECG by Adaptive Regression on Lagged Reference Signals

K. Rheinberger[†,*], T. Steinberger[†], K. Unterkofler[†], M. Baubin[‡], A. Klotz[♯], A. Amann[‡]

[†] Research Center Process and Product Engineering, University of Applied Sciences Vorarlberg, Hochschulstrasse 1, 6850 Dornbirn, Austria

[♯] Faculty of Mathematics, University of Vienna, Nordbergstrasse 15, 1090 Vienna, Austria

[‡] Department of Anaesthesiology and Critical Care Medicine, Innsbruck Medical University, Anichstrasse 35, 6020 Innsbruck, Austria

December 16, 2006

Abstract

Background and Objective: Removing cardiopulmonary resuscitation (CPR) related artifacts from human ventricular fibrillation (VF) ECG signals provides the possibility to continuously detect rhythm changes and estimate the probability of defibrillation success. This could reduce "hands-off" analysis times which diminish the cardiac perfusion and deteriorate the chance for successful defibrillations. *Methods and Results:* Our approach consists in estimating the CPR-part of a corrupted signal by adaptive regression on lagged copies of a reference signal which correlate with the CPR artifact signal. The algorithm

[*]Corresponding author: Tel.: +43 (0)5572 792 7111; Fax: +43 (0)5572 792 9510; E-mail: klaus.rheinberger@fhv.at

is based on a state-space model and the corresponding Kalman recursions. It allows for stochastically changing regression coefficients. The residuals of the Kalman estimation can be identified with the CPR-filtered ECG signal. In comparison with ordinary least-squares regression the proposed algorithm shows, for low signal-to-noise ratio (SNR) corrupted signals, better SNR improvements and yields better estimates of the mean frequency and mean amplitude of the true VF ECG signal. *Conclusions:* The preliminary results from a small pool of human VF and animal asystole CPR data are slightly better than the results of comparable previous studies which, however, not only used different algorithms but also different data pools. The algorithm carries the possibility of further optimization.

Keywords: ECG signal, cardiopulmonary resuscitation, ventricular fibrillation, artifact removal, adaptive regression, state-space model, Kalman filtering

1 Introduction

1.1 Statement of the Problem

At least 225 000 people die in the United States every year from sudden cardiac arrest before they reach a hospital, and in addition, an estimated 370 000 to 750 000 patients per year have a cardiac arrest and undergo cardiopulmonary resuscitation (CPR) during hospitalization. These statistics were published in [1] in the year 2001. Almost half of all out-of-hospital cardiac arrest patients suffer from ventricular fibrillation (VF). Presently, resuscitation is guided by a standardized protocol (the international guidelines [2, 3]) which includes only rhythm detection for decision support. As an alternative to this approach, an extended diagnostics can be devised, which is primarily based on the VF ECG and provides information on the physiological status of the individual patient. This alternative approach promotes the development of ECG-based algorithms, resulting in parameters which reflect the myocardial metabolism of the heart and its degree of resuscitability.

The international guidelines 2005 emphasize high quality CPR [4]: *Rescuers should push hard, push fast, allow full chest recoil, minimize interruptions in com-*

pressions, and defibrillate promptly when appropriate. Yet, during CPR, chest compressions and ventilations cause artifacts in the ECG [5]. In order that the rhythm detection algorithms of automatic external defibrillators work properly, a so-called "hands-off interval" is required, where CPR is stopped and the ECG is artifact-free. However, as a consequence of this, myocardial blood flow drops and the (probability for) success of a subsequent defibrillation attempt decreases [6, 7]. Thus, it would be desirable to remove CPR artifacts from the ECG continuously during CPR administration. Thereby, continuous rhythm detection could be performed minimizing "hands-off" delay times before delivering the electric countershock. Furthermore, in case of VF, CPR removal algorithms provide the possibility of continuous monitoring and determination of ECG-based parameters for estimation of defibrillation success. Such parameters rely heavily on an artifact-cleaned ECG signal. For a review of VF scoring algorithms see e.g. [8, 9]. An alternative approach consists in finding VF parameters and detection algorithms, which are insensible to CPR [10].

The human heart fibrillates at frequencies that overlap with the characteristic frequencies of CPR artifacts [11], which are determined by the chest compression rate. This is one of the reasons why CPR artifact removal presents a sophisticated signal processing problem. Furthermore, some more technical problems have to be addressed by a CPR artifact removal algorithm:

- In real emergency situations, the rates and amplitudes of chest compressions and ventilations are not constant over time.
- The CPR ECG artifacts are in general not sinusoidal and can contain high frequencies.
- The shape of the CPR ECG artifacts can change in the course of time.
- The coupling between chest compressions and the ECG can change in the course of time leading to a change in amplitude of the CPR-ECG artifacts.

Therefore we suggest that sophisticated adaptive removal algorithms are needed.

1.2 Previous Work

In contrast to the large amount of literature about algorithms for detection and analysis of VF signals, there are surprisingly only few and recent publications addressing the problem of removing CPR artifacts:

- Ruiz et al. [12] use Kalman filters assuming that the CPR artifact as well as the VF signal can be modelled by sinusoidal functions of known angular frequencies. After adding human asystole ECGs containing CPR artifacts to human artifact free VF signals they evaluated the signal-to-noise (SNR) improvements of their algorithm.

- Klotz et al. [13, 14] propose a methodology based on time-frequency methods and local coherent line removal. They evaluated their algorithms with porcine animal data by visual inspection of the spectrogram.

- The Norwegian research group of Eftestol, Husoy et al. [5, 15, 16] apply an adaptive filtering approach using additional reference signals (thoracic impedance, compression depth, etc.), which correlate with the CPR artifact signal. Besides the analysis of SNR improvement, they evaluated the performance of a shock advice algorithm before and after artifact removal [15, 16].

- Rheinberger et al. [17] model the CPR-corrupted signal by a seasonal state-space model. This allows for a stochastically changing shape of the periodic signal and also copes with time-dependent periods. Preliminary results using only a small pool of human VF and animal asystole CPR data show that the seasonal model is not as effective as models using reference signals, but it might be useful in combination with them.

1.3 Kalman state-space methods

In this article we propose Kalman state-space methods [18, 19, 20] which extend ordinary least-squares (OLS) regression. We consider Kalman methods to be appropriate for CPR artifact removal because:

- The Kalman recursions provide a numerically fast and adaptive way to compute estimates of the CPR part of the CPR corrupted signal.
- The underlying state space models include all classical time series models, can be combined in a straightforward way, and allow for integration of reference signals (thoracic impedance, compression depth, etc.).
- There exist established optimization techniques for the estimation of model parameters.

The main focus of this study lies in the presentation of the models and techniques rather than in a full-blown evaluation on an acknowledged database of signals.

2 Materials and Methods

2.1 Data and Cross-Validation

A learning data set and a different test data set of CPR corrupted signals are used, first to optimize the algorithms and then to evaluate them. Each data set consists of seven porcine asystole ECG signals during CPR and seven human artifact-free VF ECG signals which are mixed pairwise to 49 CPR-corrupted signals. Each CPR artifact recording includes an arterial blood pressure signal, lagged copies of which are used as reference signals, i.e. regressors in the regression models. All signals have a length of 10 seconds. The human ECG-data were collected using a Welch Allyn PIC 50 defibrillator.

2.2 Pre- and Postprocessing

The human artifact free VF signals are originally sampled at 375 Hz, whereas the porcine asystole CPR artifact signals and their reference signals are originally sampled at 1000 Hz. The reference signal is band-pass filtered between 0.5 and 15 Hz, detrended and normalized before using lagged copies of it as regressors. For the purpose of CPR artifact removal by means of our models, it suffices to work

at a sampling frequency of approx. 20-50 Hz, which usually covers the frequencies contained in the CPR artifact signal. This is because our models estimate the CPR artifact signal and handle the VF part as residuals. Therefore, the following procedure is applied:

1. Resample the human artifact free VF signals, denoted v, and the porcine asystole CPR artifact signals, denoted c, to a common sampling frequency such that no frequency information is lost. We used a sampling frequency of 100 Hz.

2. Normalize v and c to unit variance and scale c by an appropriate factor such that the sum $y = v + c$ has a desired SNR, where

$$\mathrm{SNR} = 10 \cdot \log_{10} \left(\frac{\mathrm{Var}(v)}{\mathrm{Var}(c)} \right).$$

   We used SNR values of -10, -5, 0, 5, and 10 dB.

3. Apply the various algorithms according to the following procedure: After detrending the mixed signal, down-sample it together with the reference signal to some sampling frequency $f \in [20, 50]$. Estimate the CPR part of the mixture by means of the chosen model and the chosen optimization procedure resulting in the signal $\hat{c}_f$.

4. In order to get an estimate $\hat{v}$ of the VF part, up-sample $\hat{c}_f$ to the common sampling frequency (100 Hz for our data), and subtract it from the mixed signal y at this sampling frequency.

2.3 Models

In many cases it is appropriate not only to regress on one reference signal, which was recorded synchronously with the CPR corrupted ECG signal, but also to regress on lagged copies of the reference signal. In this case, the OLS regression can be viewed as finding a minimum least squares filter.

2.3.1 Ordinary Least-Squares Regression Models

Let $y = (y_1, \ldots, y_T)^T$ denote observations of a CPR corrupted ECG signal and

$$(R_{t,k})_{t=1,\ldots,T}^{k=1,\ldots,M}$$

the matrix of M reference signals at T same sampling time points. OLS corresponds to finding a column vector $\hat{\beta} \in \mathbb{R}^M$, such that the Euclidean norm

$$\| y - R\hat{\beta} \|$$

is minimal for all $\beta \in \mathbb{R}^M$. The OLS estimate

$$\hat{y} := R\hat{\beta}$$

is an estimate of the CPR part of a corrupted ECG signal, whereas the regression errors, or residuals

$$e := y - \hat{y}$$

are an estimate of the artifact removed ECG signal.

We considered models differing in the sampling frequency

$$f \in \{35 \text{ Hz}, 40 \text{ Hz}, 45 \text{ Hz}\},$$

the time interval $\delta \in \{1 \text{ lag}, 2 \text{ lags}, 3 \text{ lags}\}$ between two adjacent lagged copies of the reference signal and the minimal and maximal lag

$$\begin{aligned} l_{min} &\in \{-0.20 \text{ sec}, -0.15 \text{ sec}\}, \\ l_{max} &\in \{0.25 \text{ sec}, 0.30 \text{ sec}, 0.35 \text{ sec}\}. \end{aligned}$$

Figures 1 and 2 show the result of an OLS regression on various lagged copies of the arterial blood pressure signal. Negative lags (shift towards the past) and positive lags (shift towards the future) are used. In both directions the OLS regression coef-

ficients are non-zero. Thus also future parts of the reference signal can be useful for estimating the CPR artifact part of a corrupted signal. This fact is not a hindrance for practical on-line application as it leads only to a short time delay.

2.3.2 State-Space Models and Kalman Recursions

As already pointed out, the coupling between the ECG and chest compressions as well as the shape of the CPR ECG artifacts can change in the course of time. An adaptive regression model can handle these features. We propose a state-space regression model - called ALS (Adaptive Least-Squares) - whose states are time-varying regression coefficients and whose observations are the CPR corrupted ECG signal, cf. [20]. This is a generalization of the above OLS model having constant coefficients. The observation equation of our model reads

$$\begin{aligned} Y_t &= G_t X_t + W_t, \text{ where} \\ G_t &= (R_{t,1}, \ldots, R_{t,M}), \text{ and} \end{aligned}$$

W_t is observation white noise, which models the artifact removed ECG signal and has variance σ_w^2. The upper case variables Y_t and X_t denote the random variables modelling the CPR corrupted ECG signal and the stochastic regression coefficients at time t, respectively. The state equation of our model is given by

$$X_{t+1} = F_t X_t + V_t,$$

where the time-independent state transition matrix $F_t = F$ is the $M \times M$ identity matrix. The state white noise vector V_t has covariance matrix Q. The case $Q = 0$ reproduces the OLS regression model, since the regression coefficients do not change in the course of time. A state noise covariance matrix $Q \neq 0$ allows for a dynamic evolution of the states, or, in other words, for adaptive regression coefficients.

The shortly summarize the formulas for the Kalman fixed-point smoother recursions as derived in [19]. For $T \geq n \geq t$ and fixed t, the fixed-point smoothed estimates $X_{t|n}$ (i.e. the minimum, mean squared error, linear predictor of X_t in

terms of all components of $Y_0, Y_1, \ldots, Y_n$) and error covariance matrices

$$\Omega_{t|n} := \mathrm{E}[(X_t - X_{t|n})(X_t - X_{t|n})^{\mathrm{T}}]$$

are determined by the following recursions for $n = t, t+1, \ldots$

$$\begin{aligned} X_{t|n} &= X_{t|n-1} + \Omega_{t,n} G_n^{\mathrm{T}} \Delta_n^{-1} (Y_n - G_n \hat{X}_n), \\ \Omega_{t,n+1} &= \Omega_{t,n} (F_n - \Theta_n \Delta_n^{-1} G_n)^{\mathrm{T}}, \\ \Omega_{t|n} &= \Omega_{t|n-1} - \Omega_{t,n} G_n^{\mathrm{T}} \Delta_n^{-1} G_n \Omega_{t,n}^{\mathrm{T}}, \end{aligned}$$

where $\Omega_{t,n} := \mathrm{E}[(X_t - \hat{X}_t)(X_n - \hat{X}_n)^{\mathrm{T}}]$. The 1-step predictors $\hat{X}_t := X_{t|t-1}$, their error covariance matrices $\Omega_t := \Omega_{t,t} = \Omega_{t|t-1}$, and the matrices Θ_t and Δ_t are computed in advance for every t by the following Kalman prediction recursions

$$\begin{aligned} \hat{X}_{t+1} &= F_t \hat{X}_t + \Theta_t \Delta_t^{-1} (Y_t - G_t \hat{X}_t), \\ \Omega_{t+1} &= F_t \Omega_t F_t^{\mathrm{T}} + Q_t - \Theta_t \Delta_t^{-1} \Theta_t^{\mathrm{T}}, \text{ where} \\ \Delta_t &:= G_t \Omega_t G_t^{\mathrm{T}} + R_t, \\ \Theta_t &:= F_t \Omega_t G_t^{\mathrm{T}}, \end{aligned}$$

and Δ_t^{-1} is any generalized inverse of Δ_t.

2.4 Optimization and Evaluation

First, we searched for optimal OLS regression parameters $(f, \delta, l_{min}, l_{max})$, which we then fixed for two different optimization procedures of the ALS models. We investigated three different objective functions for OLS regression models optimization, however, in order not to overcrowd the results, we considered only the optimal restored SNR parameters for evaluation on the test data set.

2.4.1 OLS Models

Using the test data set the optimal OLS model was found by a grid search. As objective functions we used the restored SNR (rSNR), which is defined as

$$\mathrm{rSNR} := 10 \cdot \log_{10} \left(\frac{\mathrm{Var}(v)}{\mathrm{Var}(v - \hat{v})} \right),$$

the difference in mean frequency (MF) of v and its estimate $\hat{v}$

$$\Delta(\mathrm{MF}) = \mathrm{MF}_v - \mathrm{MF}_{\hat{v}}$$

and the percentagewise difference in mean peak-to-trough amplitude (MA) [21] of v and $\hat{v}$

$$\Delta(\mathrm{MA}) = \frac{\mathrm{MA}_v - \mathrm{MA}_{\hat{v}}}{\mathrm{MA}_v}.$$

More precisely, for every setting of the parameters $(f, \delta, l_{min}, l_{max})$ the mean value of an objective function over all learning data sets and SNR values was computed. The MF values were computed in the frequency range $[0.1\ \mathrm{Hz}, 50\ \mathrm{Hz}]$, and the MA values were computed after band-pass filtering into the frequency range $[0.1\ \mathrm{Hz}, 25\ \mathrm{Hz}]$, cf. [21].

Only the OLS model with maximum mean rSNR was evaluated subsequently on the test data set. For each SNR the rSNR, $\Delta(\mathrm{MF})$, $\Delta(\mathrm{MA})$ values were computed for all signals in the test data set.

2.4.2 ALS Models with OLS Initialization

Using the OLS-rSNR-optimal $(f, \delta, l_{min}, l_{max})$ setting, we considered ALS models with OLS regression coefficients as initial state and an initial error covariance matrix Ω_0 which was computed using the estimator statistics of the OLS regression coefficients. Noise covariance matrices $Q = \sigma_v^2 \cdot \Omega_0$ with $\sigma_v^2 \in \{0.0015, 0.0013, 0.0011\}$ were considered, while σ_w was set to one, because the Kalman recursions only depend on the ratio Q/σ_w^2, cf. [19]. The Kalman fixed-point smoother recursions reaching one second into the future were used. For every Q the mean rSNR over all learning data

sets and SNR values was computed.

The ALS model with maximum mean rSNR was evaluated in the same way as above on the test data set.

2.4.3 ALS Models Using Reduced MLE

Using the OLS-rSNR-optimal $(f, \delta, l_{min}, l_{max})$ setting, we considered ALS models, where the optimal initial state and initial error covariance matrix, the optimal $Q = \sigma_v^2 \cdot 1_M$ and σ_w were estimated by reduced maximum likelihood estimation (rMLE), cf. [19, p.278ff]. We considered the following lower and upper bounds for the ratio $Q^* := \sigma_v^2/\sigma_w^2$

$$\{(1.5 \cdot 10^{-5}, 1.5 \cdot 10^{-4}), (1 \cdot 10^{-5}, 1 \cdot 10^{-4}), (0.5 \cdot 10^{-5}, 0.5 \cdot 10^{-4})\}.$$

Bounds for Q^* in this range force the model not to adapt the states too much over time but rather allow for large observation errors, since these model the VF part of the mixed signal. The Kalman fixed-point smoother recursions reaching one second into the future were used for every ALS model with rMLE parameters. For every Q^* the mean rSNR over all learning data sets and SNR values was computed.

The ALS model with maximum mean rSNR was evaluated in the same way as above on the test data set.

3 Results

Figure 3 compares exemplarily the true VF and CPR signals with the corresponding estimates computed with OLS and ALS methods. The ALS method accomplishes a better fit which is also reflected in a higher rSNR value.

The OLS-optimal $(f, \delta, l_{min}, l_{max})$ parameters for the learning data set are given in Table 1. The optimal state noise covariance matrix for the ALS models with OLS initialization was $Q = 0.0013^2 \cdot \Omega_0$, and the optimal lower and upper bound of Q^* was $(1 \cdot 10^{-5}, 1 \cdot 10^{-4})$ for the ALS models using rMLE optimization.

The evaluation results for the optimal rSNR parameters are shown in Figures 4,

5, and 6. Figure 4 also shows the SNR improvement which is defined as the difference rSNR − SNR. For low SNR corrupted signals, the adaptive ALS model exceeds the OLS regression model. All models underestimate the VF mean frequency by up to approx. 1.5 Hz. They overestimate the VF mean amplitude for low SNR values (approx. -15%) and underestimate it for high SNR values (approx. 5%). For high SNR corrupted signals, the adaptive ALS model performs comparably or slightly worse than the OLS regression model.

4 Discussion

Our approach consists in estimating the CPR-part of a corrupted signal by adaptive regression on lagged copies of a reference signal which correlate with the CPR artifact signal. The algorithm is based on a state-space model and the corresponding Kalman recursions. It allows for stochastically changing regression coefficients. The residuals of the Kalman estimation are identified with the CPR-filtered ECG signal.

In comparison with OLS regression the ALS algorithms show, for low SNR corrupted signals, rSNR improvements and yields better estimates of the mean frequency and mean peak-to-trough amplitude of the true VF ECG signal. Thus, the ALS model presents an improvement compared to the non-adaptive OLS model for the purpose of CPR artifact removal from VF ECG signals. This holds, in particular, because we optimized only one parameter (Q or Q^*) of the ALS model using the fixed OLS-optimal values for $(f, \delta, l_{min}, l_{max})$, which was done for computational reasons.

The mean rSNR values computed from our small pool of human artifact-free VF and porcine asystole CPR data are slightly better than the values reported by [15, 12]. These research groups, however, not only used different algorithms but also different data pools, such that the results are not truly comparable. We are planning to collaborate with these research groups using a common data pool for comparison and development of CPR removal algorithms.

The presented algorithms do not all allow for real-time CPR-filtering as for

example the efficient matching pursuit-like algorithm of Husoy et al. [15]. The simple OLS algorithm needs the complete 10 seconds signals in order to estimate the regression coefficients and subsequently compute the VF part. Likewise, the ALS models estimate the optimal initialization parameters by means of the complete signal. This, however, is not an obstruction for a possible real-time application of the proposed algorithms because they would serve as a preprocessing for rhythm detection algorithms and VF scoring algorithms. These algorithms typically also need complete segments for their analysis, e.g. Fourier transformation. Thus, the proposed CPR artifact removal methods lead to a low computational time delay.

Our optimization computes the optimal $(f, \delta, l_{min}, l_{max})$, σ_v, and Q^* values for all SNR values of the learning data set, because the SNR value is not known a priori. Yet, a closer inspection shows that the optimal $(f, \delta, l_{min}, l_{max})$, σ_v, and Q^* values depend on the SNR of the mixed signal. For the ALS models, the optimal state noise variance decreases with increasing SNR such that the states do not adapt too much over time but rather allow for large observation errors, which model the VF part of the mixed signal. Using a common state noise variance for all SNR values, thus, could be the reason for the lower performance of the ALS models at high SNR values compared to the OLS regression model. A possible improvement of the presented algorithms could therefore consist in estimating the SNR of the CPR-corrupted signal and then estimate the VF and CPR-parts by means of the SNR-optimal parameters.

In this study, we computed MF and MA values in the frequency range of [0.1 Hz, 50 Hz] and $[0.1\text{ Hz}, 25\text{ Hz}]$, respectively. Narrower frequency ranges could possible reduce the Δ(MF) and Δ(MA) values. However, this procedure can be carried out after any CPR removal algorithm. Our intent was to reveal the estimation quality of the presented algorithms in a broad frequency range.

There are several limitations of this study. Besides the limited optimization procedures applied, the results are mainly limited by the small data sets. Furthermore, only VF signals and no other shockable signals were used. To investigate the feasibility of rhythm detection algorithms during CPR also non-shockable signals should

be included, cf. [16]. An international database of human and animal ECG signals would be useful in order to evaluate the different algorithms for CPR artifact removal on a common basis. The ALS state-space model assumes that the observation noise W_t, which models the VF ECG signal, is white noise and thus uncorrelated. Figure 7 shows that a typical VF ECG signal is evidently not white noise. Thus, in a more appropriate state-space model the VF signal should be modelled more realistically, e.g. by an autoregressive process. Different objective functions can be considered. The rSNR is a common parameter to quantify the performance of a signal separation algorithm. For the practical application of CPR removal algorithms in defibrillators, however, other objective functions such as the performance of a rhythm detection algorithm or Δ(MF) and Δ(MA) could be more reasonable.

Acknowledgements

Part of this work was supported by the Austrian Science Fund (FWF) under grant L288.

References

[1] M.S. Eisenberg and T.J. Mengert. Cardiac resuscitation. *N Engl J Med*, 344(17):1304–13, 2001.

[2] Anonymous. 2005 International Consensus on Cardiopulmonary Resuscitation (CPR) and Emergency Cardiovascular Care (ECC) Science With Treatment Recommendations. *Circulation*, 112(22 Suppl):III1–136, 2005.

[3] Anonymous. 2005 American Heart Association Guidelines for Cardiopulmonary Resuscitation and Emergency Cardiovascular Care. *Circulation*, 112(24 Suppl):IV1–203, 2005.

[4] M. F. Hazinski, V. M. Nadkarni, R. W. Hickey, R. O'Connor, L. B. Becker, and A. Zaritsky. Major changes in the 2005 AHA Guidelines for CPR and ECC: reaching the tipping point for change. *Circulation*, 112(24 Suppl):IV206–11, 2005.

[5] A. Langhelle, T. Eftestol, H. Myklebust, M. Eriksen, B.T. Holten, and P.A. Steen. Reducing CPR artefacts in ventricular fibrillation in vitro. *Resuscitation*, 48(3):279–91, 2001.

[6] Y. Sato, M.H. Weil, S. Sun, W. Tang, J. Xie, M. Noc, and J. Bisera. Adverse effects of interrupting precordial compression during cardiopulmonary resuscitation. *Crit Care Med*, 25(5):733–6, 1997.

[7] T. Eftestol, K. Sunde, and P.A. Steen. Effects of interrupting precordial compressions on the calculated probability of defibrillation success during out-of-hospital cardiac arrest. *Circulation*, 105(19):2270–3, 2002.

[8] A. Amann, K. Rheinberger, and U. Achleitner. Algorithms to analyze ventricular fibrillation signals. *Curr Opin Crit Care*, 7(3):152–6, 2001.

[9] C. W. Callaway and J. J. Menegazzi. Waveform analysis of ventricular fibrillation to predict defibrillation. *Curr Opin Crit Care*, 11(3):192–9, 2005.

[10] A. Amann, U. Achleitner, H. Antretter, J. O. Bonatti, A. C. Krismer, K. H. Lindner, J. Rieder, V. Wenzel, W. G. Voelckel, and H. U. Strohmenger. Analysing ventricular fibrillation ECG-signals and predicting defibrillation success during cardiopulmonary resuscitation employing N(alpha)-histograms. *Resuscitation*, 50(1):77–85, 2001.

[11] H.U. Strohmenger, K.H. Lindner, and C.G. Brown. Analysis of the ventricular fibrillation ECG signal amplitude and frequency parameters as predictors of countershock success in humans. *Chest*, 111(3):584–9, 1997.

[12] J. Ruiz, E. Aramendi, S. Ruiz de Gauna, A. Lazkano, L.A. Leturiendo, and J.J. Gutierrez. Ventricular fibrillation detection in ventricular fibrillation signals corrupted by cardiopulmoary resuscitation artifacts. In *Proceedings of the 31. annual international conference on Computers in Cardiology*, pages 221–4, 2004.

[13] A. Klotz, H.G. Feichtinger, and A. Amann. Elimination of CPR-artefacts in VF-ECGs by time frequency methods. *Biomedizinische Technik*, 48(Ergänzungsband 1):218–219, 2003.

[14] A. Klotz, A. Amann, and H.G. Feichtinger. Removal of CPR artifacts in ventricular fibrillation ECG by local coherent line removal. In *EUSIPCO (12th European Signal Processing Conference)*, 2004.

[15] J.H. Husoy, J. Eilevstjonn, T. Eftestol, S.O. Aase, H. Myklebust, and P.A. Steen. Removal of cardiopulmonary resuscitation artifacts from human ECG using an efficient matching pursuit-like algorithm. *IEEE Trans Biomed Eng*, 49(11):1287–98, 2002.

[16] J. Eilevstjonn, T. Eftestol, S.O. Aase, H. Myklebust, J.H. Husoy, and P.A. Steen. Feasibility of shock advice analysis during CPR through removal of CPR artefacts from the human ECG. *Resuscitation*, 61(2):131–41, 2004.

[17] K. Rheinberger, M. Baubin, K. Unterkofler, and Amann A. Removal of Resuscitation Artefacts from Ventricular Fibrillation ECG Signals Using Kalman

Methods. In *Proceedings of the 32. annual international conference on Computers in Cardiology*, 32, pages 555–558, Lyon, 2005.

[18] B.D.O. Anderson and J.B. Moore. *Optimal Filtering*. Dover Publications, Inc., Mineola, New York, 2005.

[19] Peter J. Brockwell and Richard A. Davis. *Introduction to Time Series and Forecasting*. Springer, 2nd edition, 2002.

[20] M. Arnold, W.H.R. Miltner, H. Witte, R. Bauer, and C. Braun. Adaptive AR Modelling of Nonstationary Time Series by Means of Kalman Filtering. *IEEE Transactions on Biomedical Engineering*, 45(5):553–562, May 1998.

[21] A. Amann, K. Rheinberger, U. Achleitner, A.C. Krismer, W. Lingnau, K.H. Lindner, and V. Wenzel. The prediction of defibrillation outcome using a new combination of mean frequency and amplitude in porcine models of cardiac arrest. *Anesth Analg*, 95(3):716–22, 2002.

Tables

	f [Hz]	δ [lags]	l_{min} [sec]	l_{max} [sec]
rSNR	40	2	-.15	.30
Δ(MF)	35	3	-.20	.30
Δ(MA)	35	3	-.15	.25

Table 1: OLS-optimal parameters for the learning data set with respect to the objective functions rSNR, Δ(MF), and Δ(MA).

Figures

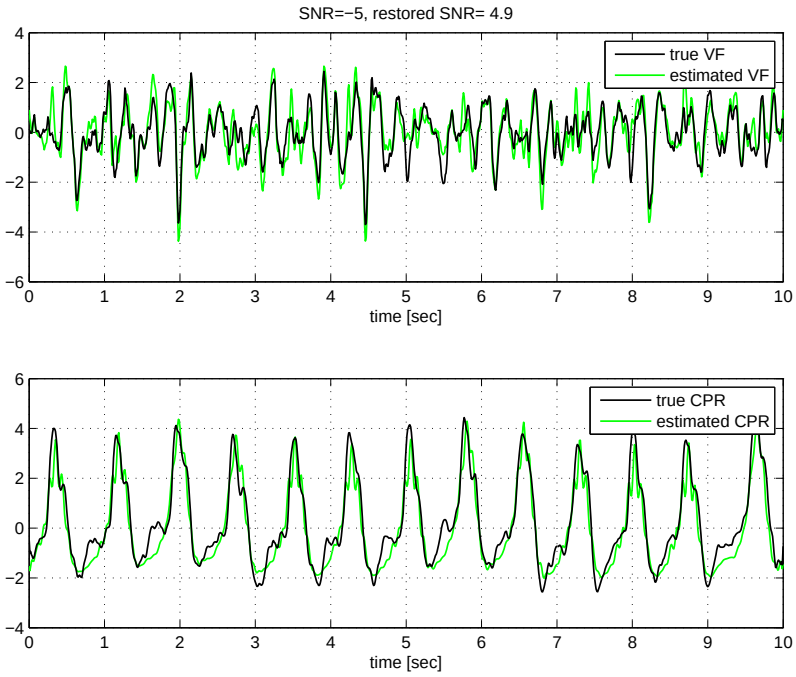

Figure 1: Results of an OLS regression of a CPR corrupted VF ECG signal on lagged copies of the arterial blood pressure signal showing the true and estimated CPR and VF part. The regression coefficients are plotted in Figure 2.

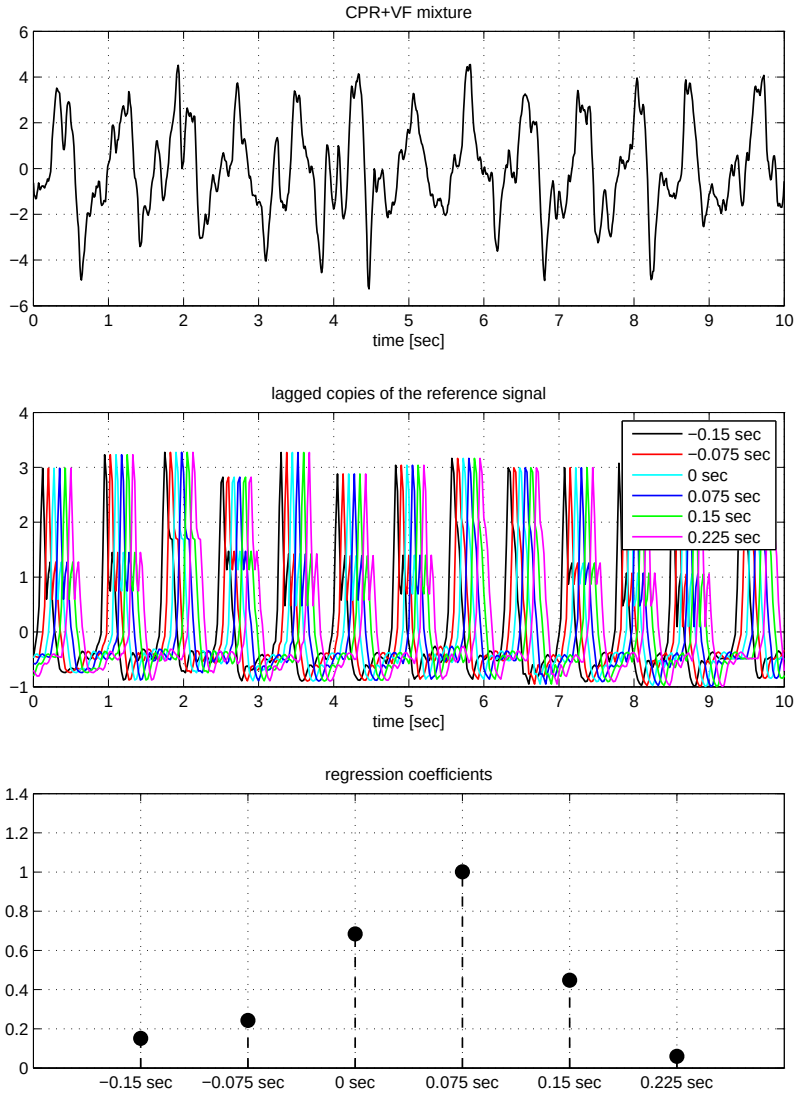

Figure 2: The CPR corrupted VF ECG signal is the sum of a CPR and a VF part. Lagged copies of the reference signal and OLS regression coefficients corresponding to Figure 1: A lag of, for example, -0.15 seconds means that the original reference signal is shifted 0.15 seconds towards the past, in other words, the reference signal values of 0.15 seconds ahead are used.

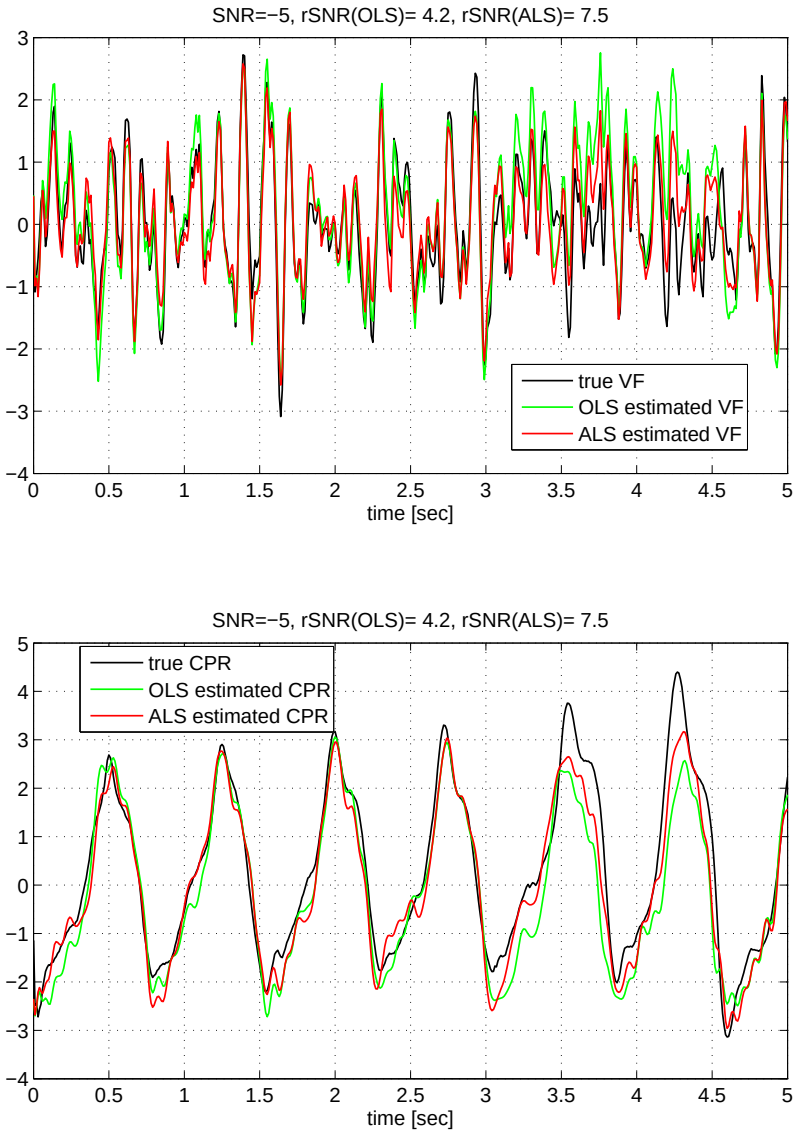

Figure 3: Comparison of true VF and CPR signals with the corresponding estimates computed with OLS and ALS methods. The ALS method accomplishes a better fit which is also reflected in a higher rSNR value.

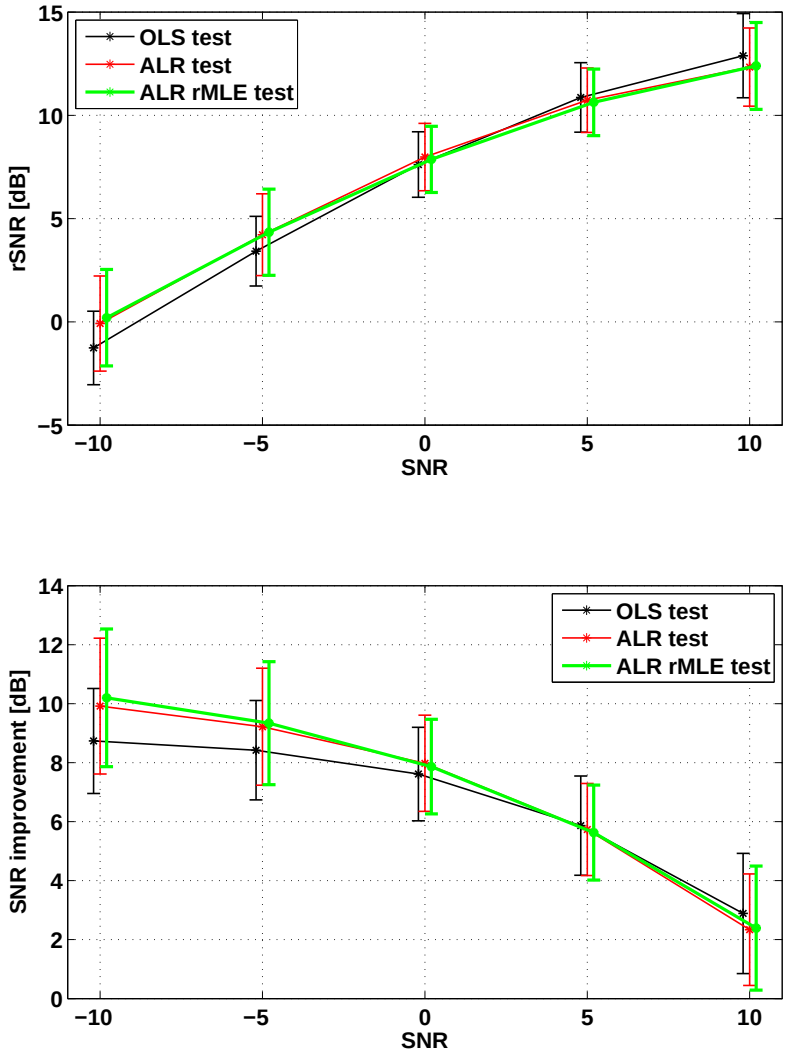

Figure 4: Evaluation results: rSNR and SNR improvement values (mean ± std) for the three models depending on the SNR of the signal mixture.

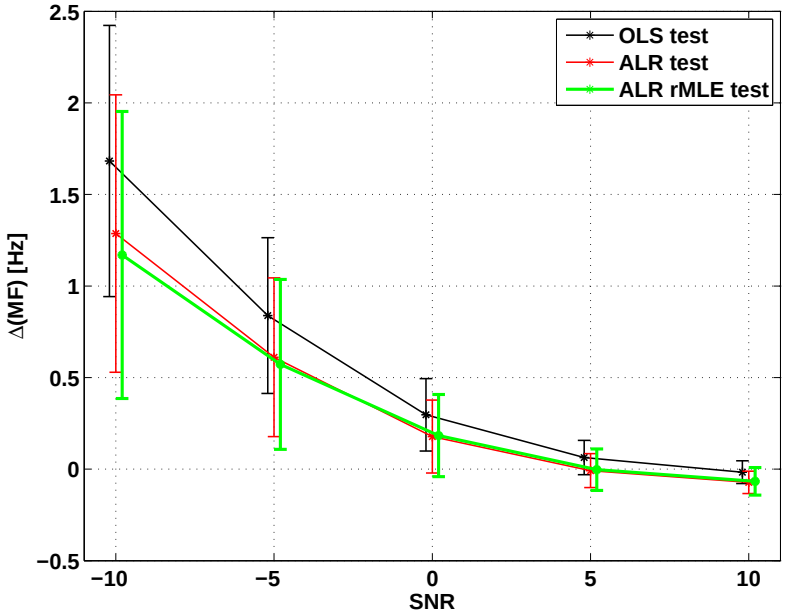

Figure 5: Evaluation results: Δ(MF) values (mean $\pm$ std) for the three models depending on the SNR of the signal mixture. The MF values were computed in the frequency range [0.1 Hz, 50 Hz], cf. [21].

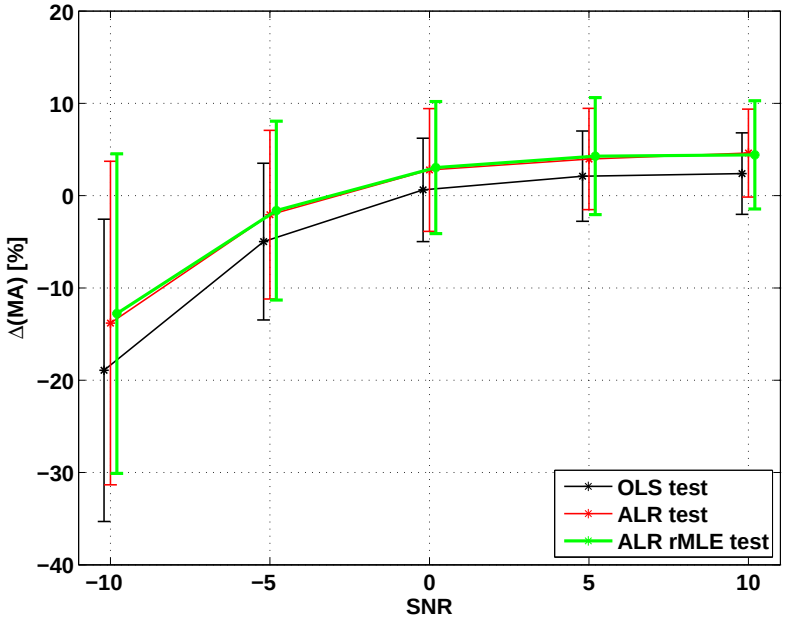

Figure 6: Evaluation results: Δ(MA) values (mean $\pm$ std) for the three models depending on the SNR of the signal mixture. The MA values were computed after band-pass filtering into the frequency range [0.1 Hz, 25 Hz], cf. [21].

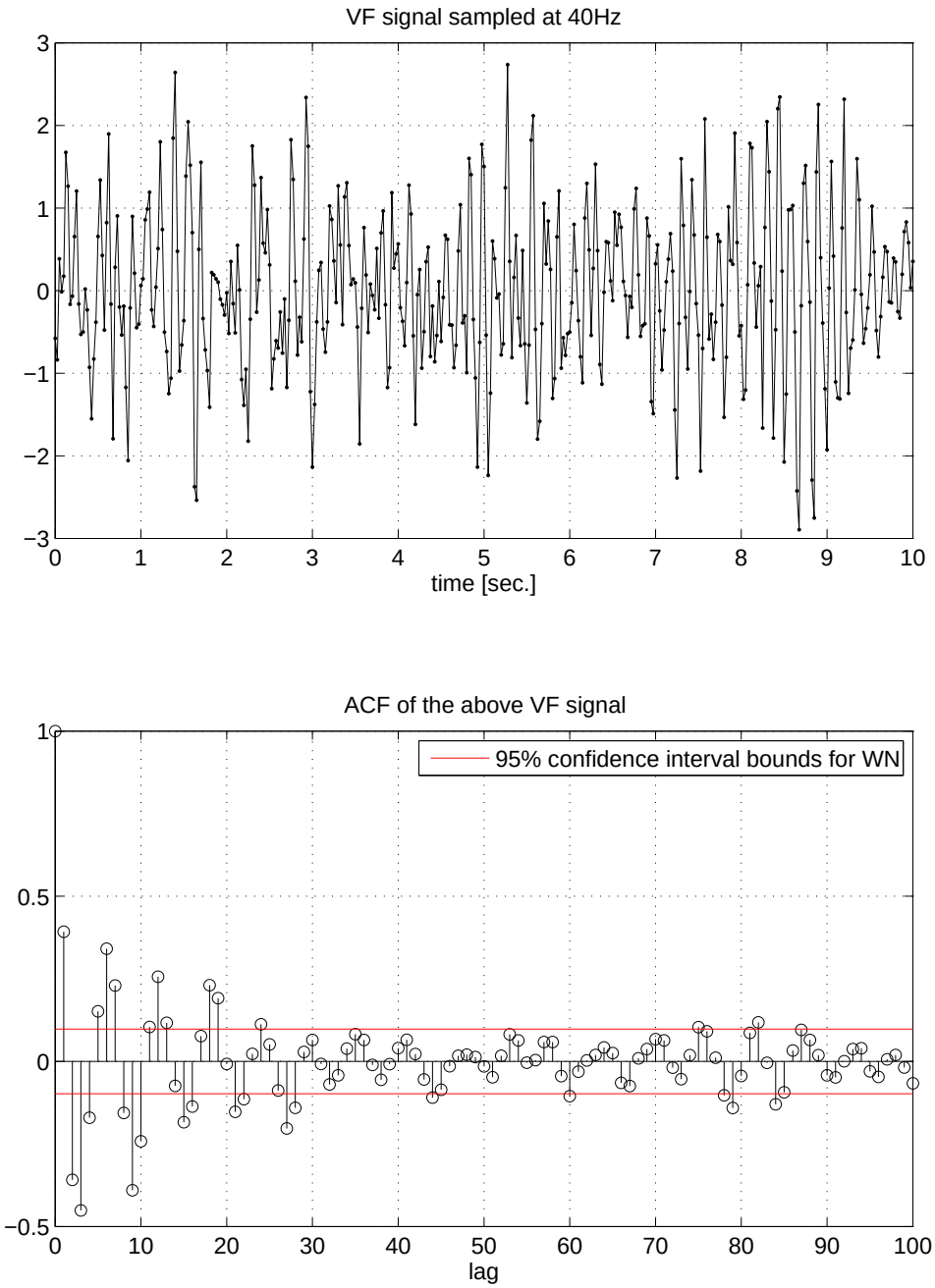

Figure 7: VF ECG signal at 40 Hz sampling frequency and corresponding autocorrelation function (ACF) including 95% confidence interval bounds for white noise (WN). The VF ECG signal is evidently not WN, cf. [19].